Neutrophil histone modification by peptidylarginine deiminase 4 is critical for deep vein thrombosis in mice

Kimberly Martinod[a,b], Melanie Demers[b,c], Tobias A. Fuchs[b,c], Siu Ling Wong[b,c], Alexander Brill[b,c], Maureen Gallant[b], Jing Hu[d], Yanming Wang[d], and Denisa D. Wagner[b,c,e,1]

[a]Immunology Graduate Program, Division of Medical Sciences, Harvard Medical School, Boston, MA 02115; [b]Program in Cellular and Molecular Medicine, Boston Children's Hospital, Boston, MA 02115; [c]Department of Pediatrics, Harvard Medical School, Boston, MA 02115; [d]Center for Eukaryotic Gene Regulation, Department of Biochemistry and Molecular Biology, Pennsylvania State University, University Park, PA 16802; and [e]Division of Hematology/Oncology, Boston Children's Hospital, Boston, MA 02115

Edited by Barry S. Coller, The Rockefeller University, New York, NY, and approved April 15, 2013 (received for review January 17, 2013)

Deep vein thrombosis and pulmonary embolism are major health problems associated with high mortality. Recently, DNA-based neutrophil extracellular traps (NETs) resulting from the release of decondensed chromatin, were found to be part of the thrombus scaffold and to promote coagulation. However, the significance of nuclear decondensation and NET generation in thrombosis is largely unknown. To address this, we adopted a stenosis model of deep vein thrombosis and analyzed venous thrombi in peptidylarginine deiminase 4 (PAD4)-deficient mice that cannot citrullinate histones, a process required for chromatin decondensation and NET formation. Intriguingly, less than 10% of *PAD4*$^{-/-}$ mice produced a thrombus 48 h after inferior vena cava stenosis whereas 90% of wild-type mice did. Neutrophils were abundantly present in thrombi formed in both groups, whereas extracellular citrullinated histones were seen only in thrombi from wild-type mice. Bone marrow chimera experiments indicated that PAD4 in hematopoietic cells was the source of the prothrombotic effect in deep vein thrombosis. Thrombosis could be rescued by infusion of wild-type neutrophils, suggesting that neutrophil PAD4 was important and sufficient. Endothelial activation and platelet aggregation were normal in *PAD4*$^{-/-}$ mice, as was hemostatic potential determined by bleeding time and platelet plug formation after venous injury. Our results show that PAD4-mediated chromatin decondensation in the neutrophil is crucial for pathological venous thrombosis and present neutrophil activation and PAD4 as potential drug targets for deep vein thrombosis.

histone citrullination | venous thromboembolism | inflammation | programmed cell death | nuclear swelling

Venous thromboembolism is associated with high mortality, with ~300,000 deaths resulting from an estimated 900,000 cases in the United States annually (1). Neutrophil extracellular traps (NETs) are produced by a cell death pathway shown to be important in innate immunity against microbes (2–5). Recently, NETs were also shown to be involved in thrombosis by binding erythrocytes and platelets (6) and in promoting coagulation by degrading tissue factor pathway inhibitor (7). Coagulation, platelets, neutrophils, and NETs have all been implicated in thrombus generation in mouse models of deep vein thrombosis (DVT) (8–10). Also, certain cancers associated with neutrophilia result in an increased propensity of circulating neutrophils to form NETs and spontaneous thrombosis (11). NETs are composed of decondensed chromatin fibers lined with antimicrobial proteins such as neutrophil elastase and myeloperoxidase (2). A proteomic analysis identified histones as the major protein component of NETs (12). Histones are highly cytotoxic to the surrounding environment into which NETs are released (13, 14) and can enhance thrombin generation (15). Histone infusion leads to rapid Weibel–Palade body (WPB) secretion from endothelial cells, promoting platelet and leukocyte adhesion and leading to accelerated thrombus generation (9). Pretreatment with DNase 1, which can degrade NETs, reduces thrombus incidence in wild-type (WT) mice (9, 10). Neutrophils play an important role, as neutrophil depletion greatly reduces thrombus weight in this model (10). Whether NETs are involved in the pathogenesis of DVT or whether they are merely a consequence of leukocyte recruitment to the thrombus is unknown. Similarly, the role of NETs in normal platelet plug formation in response to injury, where their presence was also observed (7), remains to be addressed.

Although the cellular changes occurring in the neutrophil during the process of generating neutrophil extracellular traps (NETosis) have been well described, the molecular players and processes leading to NET formation are incompletely defined. A critical step in NET formation is the decondensation of chromatin that occurs in the nucleus. Peptidylarginine deiminase 4 (PAD4) is a nuclear enzyme that converts specific arginine residues to citrulline on histone tails. Upon PAD4 activation, histones can become hypercitrullinated at histone H3Arg-8 and -17 or at histone H4Arg3 residues, resulting in the extensive chromatin decondensation that leads to nuclear delobulation and swelling during NETosis (16, 17). PAD4-deficient mice are incapable of decondensing chromatin or forming NETs (18), whereas overexpression of PAD4 is sufficient to drive chromatin decondensation to form NET-like structures in cells that normally do not form NETs (19). Because NETs are present in pathological thrombi and their dissolution by DNase 1 reduced the frequency of DVT, it was important to address the role of histone modification by PAD4 in the process of NET formation and its involvement in thrombosis.

Results

***PAD4*$^{-/-}$ Neutrophils Fail to Produce NETs in Response to Lipopolysaccharide or Ionomycin.** PAD4 is a calcium-dependent enzyme with a nuclear localization signal that distinguishes it from other PAD family members (20, 21). The enzyme is activated by Ca^{2+} (17), and therefore the calcium ionophore ionomycin was used to induce histone hypercitrullination in isolated peripheral blood murine neutrophils (Fig. 1*A*). This led to NET formation in WT and *PAD4*$^{+/-}$ neutrophils, whereas *PAD4*$^{-/-}$ neutrophils did not citrullinate histone H3 or form NETs (Fig. 1 *A* and *B*). Lipopolysaccharide (LPS) from *Klebsiella pneumoniae* was also unable to induce histone citrullination or NETs in *PAD4*$^{-/-}$ neutrophils, whereas it is a potent inducer of NETosis in WT neutrophils (Fig. 1 *A* and *B*). Moreover, immunostaining showed citrullinated histone H3 (H3Cit)-positive NETs being released from WT neutrophils, whereas in *PAD4*$^{-/-}$ neutrophils H3Cit staining was absent (Fig. 1*C*). Although *PAD4*$^{-/-}$ nuclei lost their lobulated shape characteristic of neutrophils, they did not swell, indicating that nuclear decondensation is not occurring

Author contributions: K.M., Y.W., and D.D.W. designed research; K.M., M.D., T.A.F., S.L.W., and M.G. performed research; J.H. and Y.W. contributed new reagents/analytic tools; K.M., M.D., T.A.F., S.L.W., A.B., and D.D.W. analyzed data; and K.M. and D.D.W. wrote the paper.

The authors declare no conflict of interest.

This article is a PNAS Direct Submission.

[1]To whom correspondence should be addressed. E-mail: denisa.wagner@childrens.harvard.edu.

This article contains supporting information online at www.pnas.org/lookup/suppl/doi:10.1073/pnas.1301059110/-/DCSupplemental.

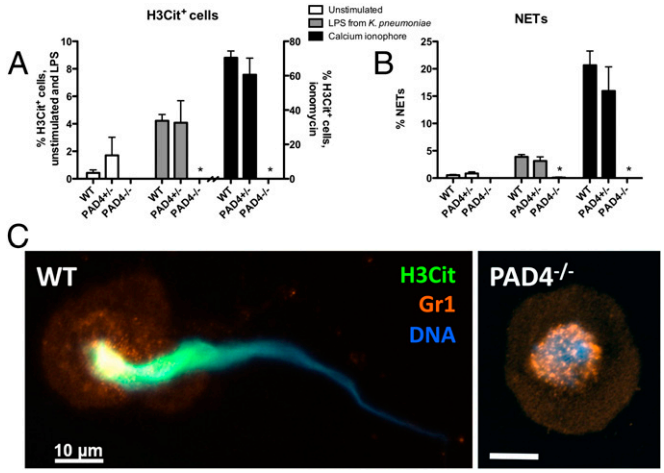

Fig. 1. PAD4 is necessary for NET formation in response to Ca^{2+} ionophore and LPS from *K. pneumoniae*. (*A* and *B*) Neutrophils isolated from WT and *PAD4*$^{+/-}$ mice became hypercitrullinated at histone H3 (*A*) and formed NETs (*B*) in response to stimulation with LPS or ionomycin for 2 h. Stimulated *PAD4*$^{-/-}$ neutrophils were negatively stained by an antibody recognizing histone H3 citrullination at residues 2, 8, and 17 and did not form NETs. (*C*) Representative micrographs of ionomycin-stimulated cells showing an H3Cit-positive NET emerging from a WT neutrophil and a condensed, delobulated nucleus in a *PAD4*$^{-/-}$ neutrophil. H3Cit staining was absent in *PAD4*$^{-/-}$ neutrophils. H3Cit, green; Gr1 antigen on plasma membrane, orange; DNA, blue. Representative of $n = 4$. (Scale bar, 10 μm.) $^*P < 0.05$.

in *PAD4*$^{-/-}$ mice and confirming that other PAD enzymes do not compensate for PAD4 deficiency in vitro. Ionomycin-induced NETosis has been shown to be independent of reactive oxygen species (22), and here we show that it is dependent on PAD4. Thus, *PAD4*$^{-/-}$ neutrophils have shown a complete inability to produce NETs (18) (Fig. 1*B*).

***PAD4*$^{-/-}$ Mice Are Protected in the Venous Stenosis Model of DVT.** Biomarkers of NETs are abundant in baboon (6) and mouse DVT (9). We performed the venous stenosis model of DVT in mice (8). Briefly, the inferior vena cava (IVC) is ligated to induce a 90% restriction in blood flow. This results in the formation of a thrombus that is macroscopically similar to human deep vein thrombi. It contains a platelet-rich white portion (distal to the ligation site) and an erythrocyte-rich red portion (proximal to the ligation site). Because PAD4-deficient mice do not form NETs in vitro, we hypothesized that NET formation would be greatly impaired in these mice during thrombosis and that this may affect thrombus formation and/or stability. *PAD4*$^{-/-}$ mice were partially protected from producing venous thrombi early after stenosis, with only 28.6% of *PAD4*$^{-/-}$ mice forming thrombi at 6 h compared with 66.7% of WT mice ($P = 0.04$) (Fig. 2*A*). Thrombi that formed in *PAD4*$^{-/-}$ mice were similar in length to WT thrombi (Fig. 2*B*). *PAD4*$^{-/-}$ mice also maintained normal platelet counts compared with control sham-operated animals and after stenosis had significantly higher platelet counts than WT mice (Fig. 2*C*). In contrast to the diffuse extracellular H3Cit pattern in thrombi previously described at 48 h (9), immunostaining revealed that the majority of H3Cit was nuclear rather than extracellular in the WT thrombi at this early time point (Fig. S1*A*), whereas H3Cit staining was not detected in *PAD4*$^{-/-}$ thrombi (Fig. S1*B*) (WT, 28.3 ± 0.75 H3Cit$^+$ cells per mm^2; *PAD4*$^{-/-}$, no H3Cit$^+$ cells detected; $n = 4$). The thrombi presented similar histological morphologies with comparable density of leukocytes as seen by H&E staining (Fig. S1*C*). To see if this early protection could be a result of delayed thrombus formation in *PAD4*$^{-/-}$ mice, we next maintained stenosis for 48 h, when the great majority of WT mice form a thrombus (8), and found that, whereas 90% of WT stenotic vessels thrombosed, fewer than 10% of *PAD4*$^{-/-}$ mice had a thrombus at this time point ($P = 0.0002$) (Fig. 2 *D* and *E*). Thrombocytopenia was associated with thrombus formation in WT mice, whereas *PAD4*$^{-/-}$ mice retained normal platelet levels (Fig. 2*F*). Thus, platelets are likely consumed by the thrombus. It is important to note that at baseline WT and *PAD4*$^{-/-}$ mice had similar platelet counts (Fig. 2*F*). The extracellular H3Cit meshwork seen in WT thrombi at 48 h postligation was again completely absent in the sole *PAD4*$^{-/-}$ thrombus, indicating also that in vivo only PAD4 modifies histone H3 to produce H3Cit (Fig. 2 *G* and *H*). Hematoxylin and eosin staining revealed many swollen neutrophil nuclei in WT thrombi, whereas the *PAD4*$^{-/-}$ thrombus contained smaller and more dense neutrophil nuclei (Fig. 2*I*). Neutrophils are abundantly present within WT thrombi at 48 h (9) and also in the only thrombus in the *PAD4*$^{-/-}$ mouse (Fig. 2*J*), suggesting that neutrophils are recruited to the *PAD4*$^{-/-}$ thrombus. NETs were absent in the single small *PAD4*$^{-/-}$ thrombus that we obtained and analyzed by immunofluorescence staining. Thus, PAD4 deficiency was highly protective in the DVT mouse model at 48 h when, in WT mice, extracellular chromatin is prominently displayed (9) (Fig. 2*G*).

Endothelial Activation and Platelet Function Are Not Affected by PAD4 Deficiency. Although PAD4 is highly expressed in neutrophils, it is also present at lower levels in many cell types, where citrullination of histones may regulate gene expression (17, 23). Therefore, it was important to establish in which cell type PAD4 was responsible for this prominent role in pathological thrombosis. First, we wanted to investigate whether endothelial release of adhesion molecules for platelets and leukocytes, von Willebrand factor (VWF) and P-selectin, from WPBs occurs normally in *PAD4*$^{-/-}$ mice. Both VWF and P-selectin were determined to be important in the stenosis model of DVT (8, 10). We turned to a time point (6 h) by which WPBs have been released, resulting in massive platelet and neutrophil adhesion to the endothelium (8). Platelet/leukocyte adhesion and aggregate formation on the IVC vessel wall were similarly present in both WT and *PAD4*$^{-/-}$ IVCs 6 h after stenosis (Fig. 3*A*) (WT, 8.97 ± 0.50; *PAD4*$^{-/-}$, 13.56 ± 2.11 leukocytes per 200 μm of vessel wall; $P = 0.10$; $n = 3$).

Another way to examine the capacity of mice to release WPBs is by infusion of activated platelets, which results in systemic WPB release from endothelial cells and consequently increases leukocyte rolling in veins (24). Leukocyte rolling occurred in both WT and *PAD4*$^{-/-}$ mice to a similar extent over baseline 2 h after activated platelet infusion (Fig. 3 *B* and *C*), an interaction that is dependent on endothelial P-selectin and P-selectin glycoprotein ligand-1 (PSGL-1) on leukocytes (24). Plasma VWF levels were similarly elevated in WT and *PAD4*$^{-/-}$ mice 2 h after platelet infusion (WT, 154.6 ± 8.24%; *PAD4*$^{-/-}$, 140.0 ± 21.8% of control pooled plasma; $n = 4$, $P = 0.56$). Taken together, the protection of *PAD4*$^{-/-}$ mice in DVT is not due to a defect in endothelial activation leading to VWF and P-selectin release, nor is it due to a defect in the initial leukocyte and platelet adhesion to the vessel wall that is essential for thrombus initiation in venous stenosis (8, 10).

Because PAD4 could be expressed in megakaryocytes and thus affect the properties of platelets, we next evaluated the platelets from *PAD4*$^{-/-}$ mice. As Fig. 2*F* shows, at baseline the platelet count in *PAD4*$^{-/-}$ mice was normal. Platelets isolated from *PAD4*$^{-/-}$ mice aggregated normally in response to low and high doses of thrombin (Fig. 3 *D* and *E*). This shows that, in general, platelet activation, granule secretion, and integrin activation are not affected in these mice. We then examined in vivo models in which platelets respond to injury by forming a platelet plug: tail bleeding time and the ferric chloride model of thrombosis. Tail-tip transection results in severing of both veins and artery, and the rapid cessation of blood flow depends on platelet function and coagulation. Time to cessation of bleeding was similar in WT and *PAD4*$^{-/-}$ mice (Fig. 3*F*), indicating that these mice have normal hemostatic potential. In the venous stenosis model, flow restriction leads to WPB secretion potentially due to local hypoxia (25), resulting in platelet–leukocyte interactions with the

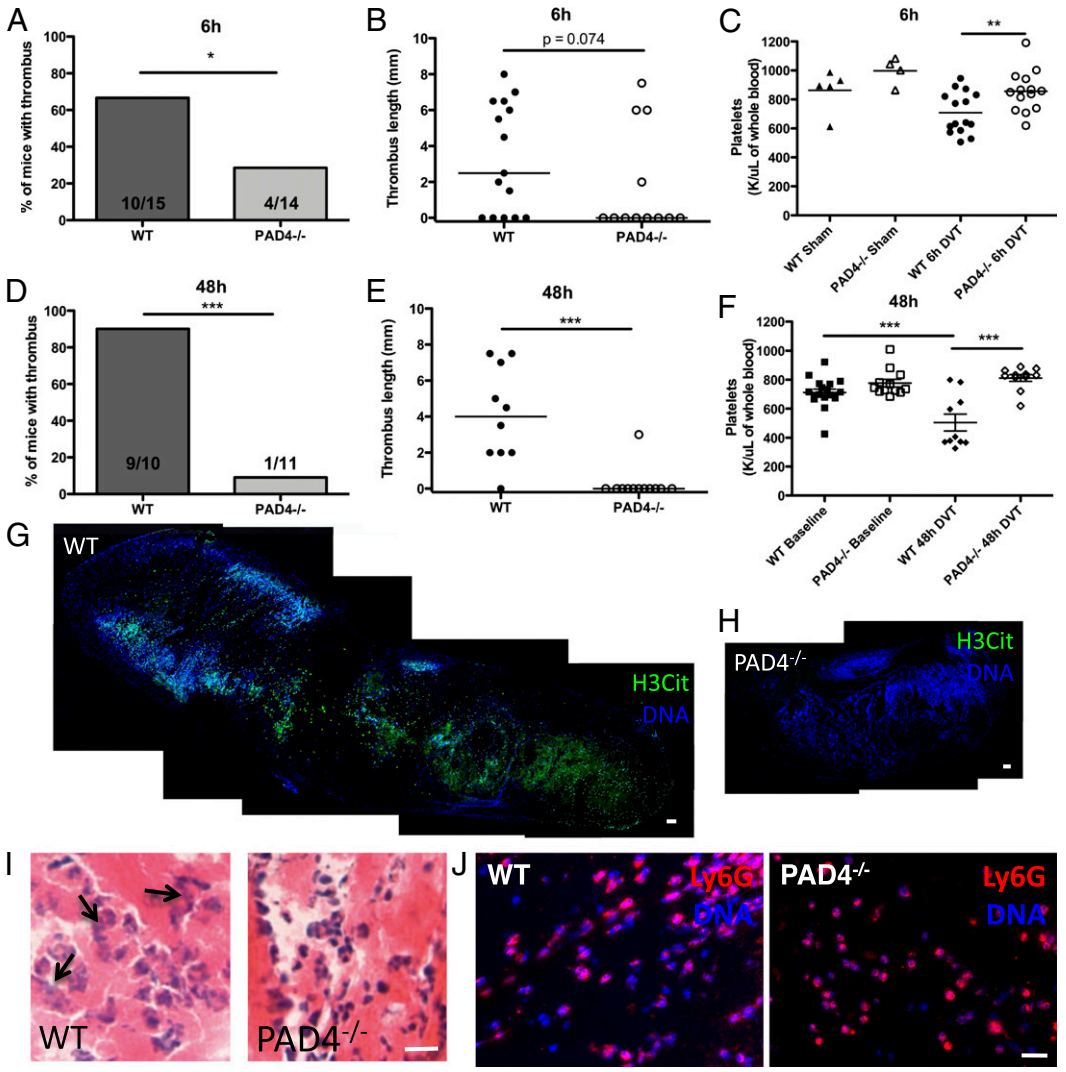

Fig. 2. *PAD4*$^{-/-}$ mice are protected from DVT, especially at 48 h after stenosis. (*A* and *B*) *PAD4*$^{-/-}$ mice were less likely to form thrombi at 6 h than WT mice. (*C*) Platelet count is decreased in WT compared with *PAD4*$^{-/-}$ mice after 6 h in the venous stenosis model. (*D* and *E*) At 48 h, only one small thrombus was present in a *PAD4*$^{-/-}$ mouse, whereas all but one of the WT mice had thrombi. (*F*) WT and *PAD4*$^{-/-}$ mice have similar platelet counts before stenosis ("Baseline"). WT mice are thrombocytopenic at 48 h, whereas platelet counts remain stable in *PAD4*$^{-/-}$ mice. (*G* and *H*) Composite image of a section from an entire thrombus collected at 48 h showing diffuse, extracellular H3Cit (green) staining in a WT mouse (*G*), which is completely absent in the sole thrombus from a *PAD4*$^{-/-}$ mouse (*H*). Hoechst staining of DNA is shown in blue and shows extensive presence of leukocytes in both thrombi. (Scale bars, 100 μm.) (*I*) H&E staining of 48 h thrombi shows less dense nuclear staining and diffuse, likely extracellular, DNA (arrows) in WT thrombi compared with dense nuclei found in the *PAD4*$^{-/-}$ thrombus. (Scale bar, 20 μm.) (*J*) Thrombi collected from WT mice or the *PAD4*$^{-/-}$ mouse that formed a thrombus 48 h after IVC stenosis showed an abundance of neutrophils by Ly6G immunostaining (red). (Scale bar, 20 μm.) DNA is shown in blue. **P* < 0.05, ***P* < 0.01, ****P* < 0.001.

endothelium. In the ferric chloride model, by contrast, oxidative injury removes the endothelium and exposes circulating blood to the subendothelial matrix (26). Platelets bind to the subendothelium via glycoprotein Ib (GPIb), integrins, and glycoprotein VI (GPVI) and then become activated and aggregate via integrin receptors (27). We visualized thrombus formation in $FeCl_3$-injured mesenteric venules using intravital microscopy and found that *PAD4*$^{-/-}$ mice formed occlusive thrombi with similar kinetics (Fig. 3*G*) and thrombus morphologies (Fig. 3*H*) as WT mice. Thus, we have no evidence that PAD4 or NETs play a significant role in hemostasis in healthy mice. For platelet plug formation in the injured veins, coagulation is likely driven by vessel wall tissue factor. Here the enhancement of coagulation and thrombosis by NETs may not be necessary.

Neutrophil PAD4 Is a Key Player in Pathological Thrombus Formation. To assess whether the influence of PAD4 was of hematopoietic origin, we generated bone marrow (BM) chimeras by infusing WT or *PAD4*$^{-/-}$ BM cells into lethally irradiated WT recipients. Both groups of mice recovered body mass with similar kinetics (Fig. S2*A*). To test the chimerism, we stimulated leukocytes from whole blood after red blood cell (RBC) lysis with ionomycin and found that the *PAD4*$^{-/-}$ BM chimeras failed to hypercitrullinate arginine residues at histone H3 (Fig. S2 *B* and *C*). Similar to the thrombus formation frequencies in WT and *PAD4*$^{-/-}$ mice, a majority (six of seven) of WT BM chimeras produced thrombi after 48 h of stenosis, whereas only one of the seven *PAD4*$^{-/-}$ BM chimeras formed a small thrombus (Fig. 4 *A* and *B*). The H3Cit pattern within thrombi paralleled the results seen in WT and *PAD4*$^{-/-}$ mice, with extracellular H3Cit present in the thrombi of WT BM chimeras but H3Cit staining absent in the *PAD4*$^{-/-}$ BM chimera thrombus (Fig. S2 *D* and *E*). WT BM chimeras became thrombocytopenic 48 h poststenosis, whereas *PAD4*$^{-/-}$ BM chimeras maintained normal platelet counts (Fig. 4*C*).

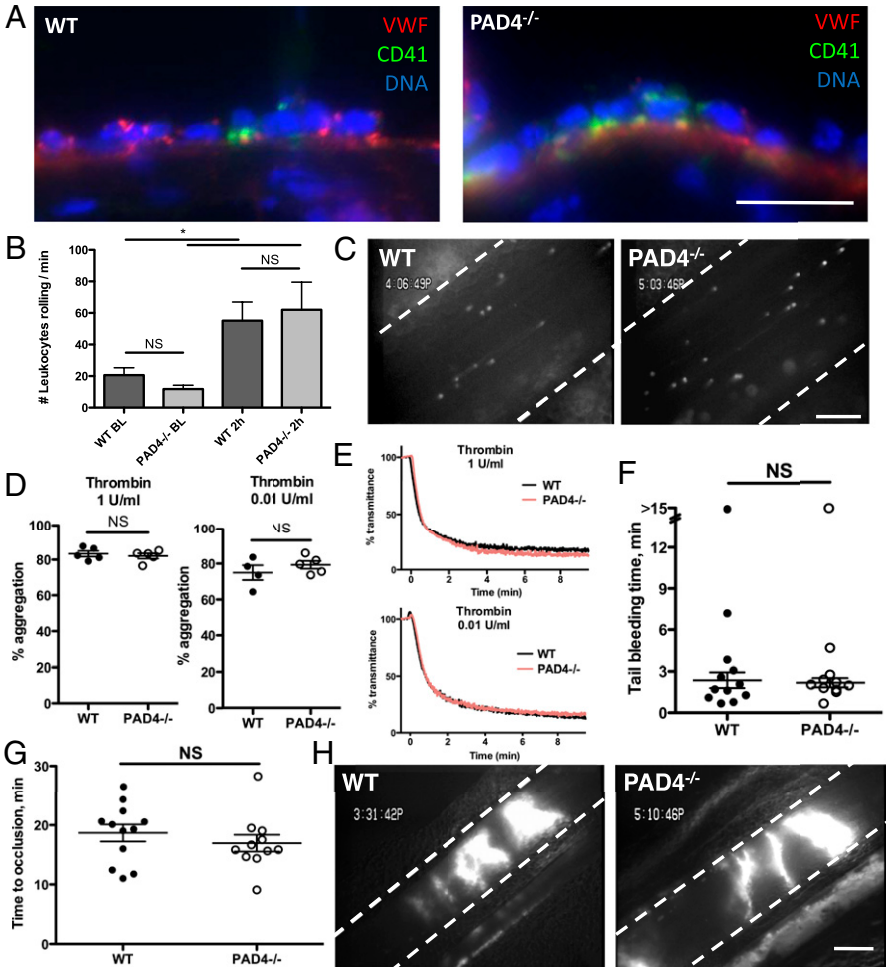

Fig. 3. Normal adhesive interactions among platelets, leukocytes, and endothelium in *PAD4*$^{-/-}$ mice. (*A*) Representative images of platelets, leukocytes, and platelet–leukocyte aggregates on endothelium in WT (*Left*) or *PAD4*$^{-/-}$ (*Right*) IVCs collected 6 h after ligation. VWF, red; CD41 (platelets), green; DNA, blue. $n = 3$–4. (Scale bar, 20 μm.) (*B* and *C*) Activated platelets were infused into WT or *PAD4*$^{-/-}$ mice. (*B*) Leukocyte rolling was assessed in mesenteric venules by counting the number of cells crossing a defined line per minute. Baseline leukocyte rolling was determined in untreated mice. $n = 4$–6. (*C*) Representative still images from intravital microscopy movies showing numerous rolling leukocytes 2 h after activated platelet infusion in WT or *PAD4*$^{-/-}$ mice. (Scale bar, 100 μm.) (*D* and *E*) Aggregometry of washed platelets stimulated with thrombin at 1 or 0.01 U/mL. (*D*) Maximum aggregation was similar between WT and *PAD4*$^{-/-}$ mice. (*E*) Representative traces showing similar kinetics of aggregation between platelets from WT and *PAD4*$^{-/-}$ mice. Red line, *PAD4*$^{-/-}$; black line, WT. $n = 4$–5. (*F*) A 2-mm tail segment was transected and bleeding was monitored for 15 min. The time to the first cessation in bleeding was recorded for each mouse. One mouse from each group failed to stop bleeding, and these mice were determined to be statistical outliers using Grubb's test and excluded from means. (*G* and *H*) Venous thrombosis after injury. Mesenteric venules were externalized and injured with application of 10% $FeCl_3$-soaked filter paper for 5 min. (*G*) Time to vessel occlusion was measured and found to be similar in WT and *PAD4*$^{-/-}$ mice. (*H*) Representative images of occlusive thrombi formed in WT (*Left*) or *PAD4*$^{-/-}$ mice (*Right*). $n = 11$–12. (Scale bar, 200 μm.)

As PAD4 is expressed by other leukocytes in addition to neutrophils (28, 29) that may enter the thrombus, we investigated whether the infusion of WT neutrophils could rescue thrombosis in *PAD4*$^{-/-}$ mice at 48 h. Infusing 4–5 × 10^6 isolated WT BM neutrophils into *PAD4*$^{-/-}$ mice restored thrombus generation (Fig. 4 *D* and *E*). Although a significant lowering of platelet count was not achieved by neutrophil infusion (Fig. 4*F*), mice that had formed a thrombus in either WT and *PAD4*$^{-/-}$ recipients did, however, have a significant decrease in platelet count compared with baseline levels (Fig. S3). Infused neutrophils were of >95% purity as assessed by Wright–Giemsa staining (Fig. S4*C*). The thrombi from neutrophil-infused *PAD4*$^{-/-}$ mice contained large numbers of Ly6G$^+$ neutrophils, whereas F4/80$^+$ monocytes/macrophages were rarely seen within all thrombi examined (Fig. S4 *A*, *B*, and *D*). Thrombi were analyzed by immunofluorescence, and extracellular H3Cit staining was present within both WT and *PAD4*$^{-/-}$ recipient thrombi after WT neutrophil infusion (Fig. 4 *G* and *H*), indicating that the WT neutrophils were incorporated and produced NETs in the thrombus scaffold in *PAD4*$^{-/-}$ recipient mice. Therefore, PAD4 within neutrophils is important for formation of stable thrombi in large veins, as the defect in thrombosis in *PAD4*$^{-/-}$ mice can be rescued by supplementation with WT neutrophils.

Discussion

For more than 150 y, the conditions of hypercoagulable state, hypoxia due to flow disturbance such as in valves or stasis, and vascular activation were recognized as the main players in DVT (30). Only recently has the active contribution of blood cells to DVT begun to be appreciated. First, the complex role of inflammatory cells was recognized in that they promote thrombosis, for example, through production of tissue factor, and also contribute to thrombus resolution (31). Second, the important role of platelets in DVT has been described in animal models and human trials (9, 32, 33). Venous pathological thrombi were thought to be formed by fibrin and trapped RBCs, and the main treatment in humans is still anticoagulation. It is now clear that pathological thrombus formation and stabilization are much more complex, with many platelets and leukocytes present, and even the RBCs may not be trapped but rather actively recruited to the thrombus by NETs (6). Thus, new treatment options are being revealed.

Here we reveal a different facet of DVT—the importance of neutrophil posttranslational modification and chromatin decondensation, factors dramatically influencing outcome of stenosis-induced DVT in mice. The enzyme PAD4 allows for dissociation of heterochromatin protein 1-β (19), affects linker histone H1 (16), and reduces the positive charge of histones by arginine citrullination, thus allowing nucleosomes to unravel and chromatin to be expelled from the swollen nuclei. Absence of NETosis resulted in the formation of fewer thrombi in *PAD4*$^{-/-}$ mice early after the flow disturbance/hypoxia onset with almost no thrombi by 48 h. Here we describe DVT as a noninfectious model in which the *PAD4*$^{-/-}$ mice are affected, and, surprisingly, to date this is the strongest phenotype described in these mice (18, 34, 35).

We have demonstrated that PAD4 deficiency does not perturb initial vessel wall activation and platelet–leukocyte adhesion. Also, platelets from PAD4 knockout mice are fully functional and able to produce platelet plugs like WT platelets. The low incidence of DVT in *PAD4*$^{-/-}$ mice is largely caused by a lack of PAD4 in neutrophils as WT neutrophils could rescue the DVT

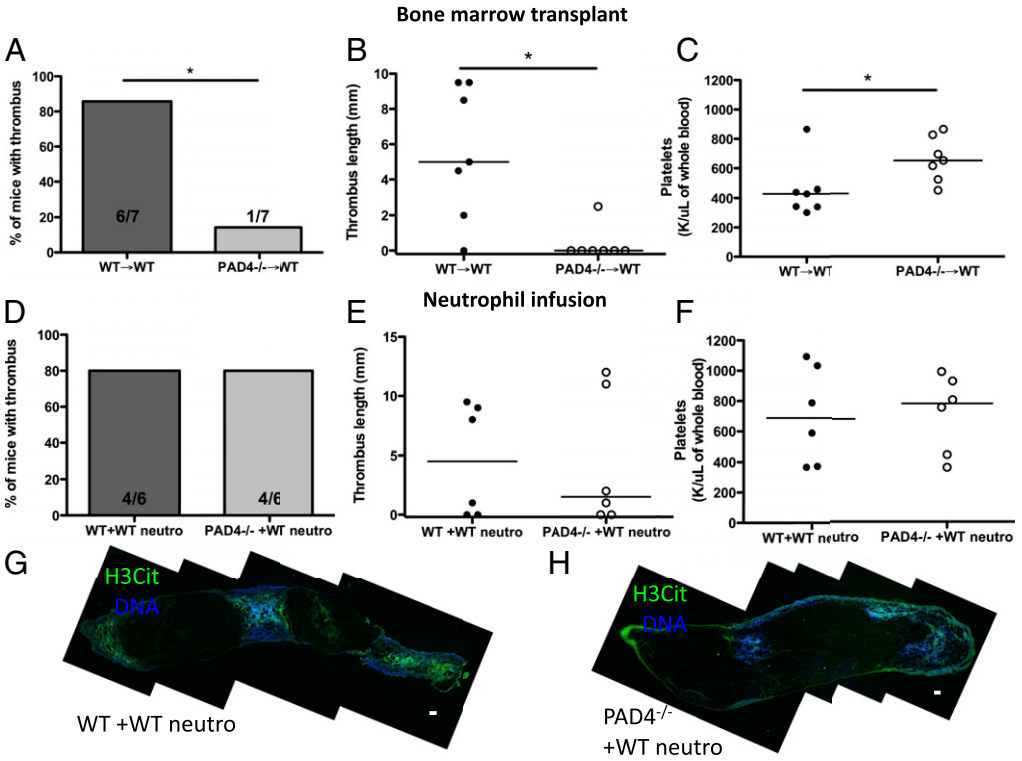

Fig. 4. Venous thrombosis depends on the presence of PAD4 in neutrophils. (*A*–*C*) Chimeric mice were generated by infusing WT or *PAD4*$^{-/-}$ BM cells into lethally irradiated WT recipients and later subjected to 48 h of IVC stenosis. (*A*) Percentage of BM chimeras that produced thrombi. (*B*) Length of thrombi. (*C*) Platelet counts in BM chimeras 48 h after DVT surgery. WT→WT BM chimeras became thrombocytopenic, whereas *PAD4*$^{-/-}$→WT BM chimeras maintained normal platelet counts. (*D*–*H*) WT or *PAD4*$^{-/-}$ mice received an i.v. infusion of 4–5 × 10^6 WT neutrophils immediately before DVT surgery and 2–2.5 × 10^6 neutrophils at 24 h. (*D* and *E*) A majority (80%) of both WT and *PAD4*$^{-/-}$ mice formed thrombi after the infusion of WT neutrophils. (*F*) Similar platelet counts were measured 48 h after IVC ligation in WT and *PAD4*$^{-/-}$ mice infused with WT neutrophils. (*G* and *H*) Composite images of thrombi collected from mice infused with WT neutrophils. H3Cit-positive nuclei and extracellular staining was detected in WT (*G*) and *PAD4*$^{-/-}$ (*H*) thrombi, indicating that the infused WT neutrophils integrated into the *PAD4*$^{-/-}$ thrombus. H3Cit, green; DNA, blue. Representative of $n = 4$. (Scale bar, 100 μm.) *$P < 0.05$.

process. The protection in *PAD4*$^{-/-}$ mice from DVT is due to the failure of neutrophils to form NETs as the *PAD4*$^{-/-}$ neutrophils interact properly with the vessel wall and are present in the rare thrombi that form in *PAD4*$^{-/-}$ veins. Our observation of less extracellular H3Cit in WT thrombi at 6 h than at 48 h (Fig. S1 and Fig. 2) fits well with the report of von Brühl and colleagues (10) showing that neutrophils begin to throw NETs by 3 h in this DVT model, but the prominent diffuse staining pattern of NETs is present only later, at 48 h. Thus, NETs compose a crucial part of the pathologic thrombus scaffold, and the lack of NET formation results in fewer thrombi early on that appear not to be sustained over time.

Our observations help to pinpoint the importance of neutrophils and NETs in thromboembolic disease. Inhibitors of neutrophil activation in the thrombus, inhibitors of PAD4 activation, or inhibitors of NET release would all impact DVT outcome. Therapeutic interventions combining both DNases and proteolytic enzymes may improve thrombolysis in patients with DVT. In addition, specific PAD4 inhibitors are not likely to impair hemostasis or neutrophil function in thrombus resolution. Thus, a better understanding of the complexity of pathological thrombosis, including the process of chromatin decondensation in neutrophils, will bring us closer to devising more effective and targeted treatments.

Materials and Methods

Mice. Experimental procedures in this study were reviewed and approved by the Institutional Animal Care and Use Committee of Boston Children's Hospital (protocol nos. 11–03-1919, 11–04-1848, 11–03-1941). WT mice were purchased from Jackson Laboratory. *PAD4*$^{-/-}$ mice have been recently backcrossed to C57BL/6J for seven or more generations.

Neutrophil Isolation for in Vitro NET Assays. Peripheral blood was collected via the retroorbital venous plexus, and neutrophils were isolated from 6- to 10-wk-old male or female WT, *PAD4*$^{+/-}$, or *PAD4*$^{-/-}$ mice as previously described (11). Cells were routinely assessed to be >90% pure by Wright–Giemsa stain. Neutrophils in RPMI/Hepes were allowed to adhere at 37 °C in 5% CO_2 to glass-bottom plates for 20 min before stimulation with 10 μg/mL LPS from *K. pneumoniae* (Sigma) or 4 μM ionomycin (Invitrogen). After 2 h, cells were fixed in 2% (vol/vol) paraformaldehyde.

Venous Stenosis Model. Venous stenosis experiments were performed as previously described (8). Please see *Supporting Information* for more detailed methods.

Immunostaining and Fluorescence Microscopy. Fixed cells or tissue sections were washed with PBS and permeabilized (0.1% Triton X-100, 0.1% sodium citrate) for 10 min at 4 °C. Samples were blocked with 3% (wt/vol) BSA for 90 min at 37 °C, rinsed, and then incubated overnight at 4 °C or for 1 h at 37 °C in antibody dilution buffer containing 0.3% BSA, 0.1% Tween-20, and either rabbit antihistone H3 (citrulline 2, 8, 17) (0.3 μg/mL, ab5103; Abcam), rat anti-Gr1 (0.5 μg/mL, clone RB6-8C5; eBioscience), rat anti-Ly6G (0.5 μg/mL, clone 1A8; Biolegend), or rat anti-F4/80 (1:250, ab16911; Abcam). After several washes, samples were incubated for 2 h at room temperature in antibody dilution buffer containing Alexa Fluor-conjugated secondary antibodies in 0.3% BSA in PBS: goat anti-rat Ig (IgG) (Alexa555, 2 μg/mL), donkey anti-rabbit IgG (Alexa488, 1.5 μg/mL), or donkey anti-sheep IgG (Alexa568, 2 μg/mL; Invitrogen). DNA was counterstained with 1 μg/mL Hoechst 33342 and slides were coverslipped with Fluoromount gel (Electron Microscopy Sciences). Fluorescent images were acquired using an Axiovert 200 widefield fluorescence microscope (Zeiss) in conjunction with an Axiocam MRm monochromatic CCD camera (Zeiss) and analyzed with Zeiss Axiovision software. All channels were acquired in grayscale and pseudocolored using Zeiss Axiovision or ImageJ software (National Institutes of Health). Exposure times are identical between

WT and *PAD4*$^{-/-}$ thrombi or neutrophils. Composite images were generated with the MosaicJ plugin (36) for ImageJ software.

Platelet Counts. Whole blood was collected via the retroorbital sinus into EDTA-coated capillary tubes. Twenty-five μL of blood was analyzed by a Hemavet 950FS (Drew Scientific) for complete blood counts.

Platelet Aggregation. Murine blood was collected in 10% (vol/vol) sodium citrate [3.2% (wt/vol)] and centrifuged at 800 × *g* for 10 min. Platelet-rich plasma was collected, and supplemented with prostacyclin in Tyrode's buffer. Platelets were washed and resuspended in Tyrode's buffer and incubated at 37 °C. Platelets (2.5×10^5/μL) were analyzed using a Chronolog Platelet aggregometer. Thrombin (1 or 0.01 U/mL) in the presence of calcium chloride was used as an agonist for aggregation, and samples were analyzed for at least 10 min.

Tail Bleeding Time. Six- to 8-wk-old male or female C57BL/6J or *PAD4*$^{-/-}$ mice were anesthetized using 2.5% (vol/vol) tribromoethanol (300 mg/kg) administered intraperitoneally. A 2-mm segment of the tail tip was transected using a single-edge razor blade, and the tail was immediately submersed in 37 °C PBS. Tail bleeding was monitored for 15 min, and the time to stop was recorded when bleeding had stopped for more than 30 s. All mice were euthanized immediately at the end of the observation period.

$FeCl_3$-Induced Mesenteric Venous Thrombosis. Three- to 4-wk-old C57BL/6J or *PAD4*$^{-/-}$ male mice were anesthetized using 2.5% (vol/vol) tribromoethanol (300 mg/kg) administered i.p., and the level of anesthesia was verified by lack of response to footpad squeeze. Rhodamine 6G was given via retroorbital injection to fluorescently label platelets and leukocytes. A midline incision was performed, and the intestines externalized to reveal mesenteric vessels. A single venule of between 200 to 300 μm in diameter was visualized for each mouse (WT mice, 222.2 ± 20.6 μm; *PAD4*$^{-/-}$ mice, 239.0 ± 44.6 μm). A 1- × 3-mm piece of filter paper was soaked in 10% ferric chloride, gently placed on the vessel for 5 min, and then removed. Occlusion time was noted for each mouse. Vessels were considered occluded when blood flow had stopped for at least 10 s.

Bone Marrow Chimera Preparation. Four-week-old C57BL/6J males were lethally irradiated with 1,100 rad and immediately given an i.v. injection of at least 1×10^7 bone marrow cells from either WT or *PAD4*$^{-/-}$ mice. See *Supporting Information* for detailed methods.

Neutrophil Infusion. Neutrophil adoptive transfer studies were performed as previously described (37). BM neutrophils were isolated from 6- to 8-wk-old C57BL/6J WT mice using a Percoll (GE Healthcare Life Sciences) gradient and rapid hypotonic lysis. Bone marrow was flushed out of tibias and femurs using a 30-G needle into cold RPMI. Cells were pelleted, resuspended in PBS, and layered onto a Percoll gradient containing 78%/69%/52% (vol/vol) Percoll. Cells at the 78%/69% interface were collected and subjected to hypotonic lysis. Cells were counted using a hemacytometer and resuspended in RPMI. Purity was assessed by Wright–Giemsa staining, which was determined to be >95% neutrophils. Cells ($4–5 \times 10^6$) were injected i.v. through the retroorbital sinus immediately before DVT surgery. A second i.v. neutrophil infusion of $2–2.5 \times 10^6$ neutrophils was given at 24 h. Mice were euthanized at 48 h, and any resulting thrombi were harvested for analysis.

Statistics. Data are presented as means ± SEM unless otherwise noted and were analyzed using a two-sided Student *t* test or Mann–Whitney *U* test. Thrombus frequencies were analyzed using χ^2 tests of contingency tables. All analyses were performed using GraphPad Prism software (Version 5.0). Results were considered significant at $P < 0.05$ (*$P < 0.05$, **$P < 0.01$, ***$P < 0.001$).

ACKNOWLEDGMENTS. We thank Tanya N. Mayadas for helpful discussions and for the method of neutrophil infusion, Stephen M. Cifuni for expert technical assistance, and Lesley Cowan for assistance in manuscript preparation. This work was supported by the National Heart, Lung, and Blood Institute of the National Institutes of Health Grants R01 HL095091, R01 HL041002, and HL102101 (to D.D.W.), and R01 CA136856 (to Y.W.). K.M. was supported in part by a research grant from GlaxoSmithKline.

1. Raskob GE, Silverstein R, Bratzler DW, Heit JA, White RH (2010) Surveillance for deep vein thrombosis and pulmonary embolism: Recommendations from a national workshop. *Am J Prev Med* 38(4, Suppl):S502–S509.
2. Brinkmann V, et al. (2004) Neutrophil extracellular traps kill bacteria. *Science* 303(5663):1532–1535.
3. Brinkmann V, Zychlinsky A (2012) Neutrophil extracellular traps: Is immunity the second function of chromatin? *J Cell Biol* 198(5):773–783.
4. Fuchs TA, et al. (2007) Novel cell death program leads to neutrophil extracellular traps. *J Cell Biol* 176(2):231–241.
5. Yipp BG, et al. (2012) Infection-induced NETosis is a dynamic process involving neutrophil multitasking in vivo. *Nat Med* 18(9):1386–1393.
6. Fuchs TA, et al. (2010) Extracellular DNA traps promote thrombosis. *Proc Natl Acad Sci USA* 107(36):15880–15885.
7. Massberg S, et al. (2010) Reciprocal coupling of coagulation and innate immunity via neutrophil serine proteases. *Nat Med* 16(8):887–896.
8. Brill A, et al. (2011) von Willebrand factor-mediated platelet adhesion is critical for deep vein thrombosis in mouse models. *Blood* 117(4):1400–1407.
9. Brill A, et al. (2012) Neutrophil extracellular traps promote deep vein thrombosis in mice. *J Thromb Haemost* 10(1):136–144.
10. von Brühl ML, et al. (2012) Monocytes, neutrophils, and platelets cooperate to initiate and propagate venous thrombosis in mice in vivo. *J Exp Med* 209(4):819–835.
11. Demers M, et al. (2012) Cancers predispose neutrophils to release extracellular DNA traps that contribute to cancer-associated thrombosis. *Proc Natl Acad Sci USA* 109(32): 13076–13081.
12. Urban CF, et al. (2009) Neutrophil extracellular traps contain calprotectin, a cytosolic protein complex involved in host defense against Candida albicans. *PLoS Pathog* 5(10):e1000639.
13. Xu J, et al. (2009) Extracellular histones are major mediators of death in sepsis. *Nat Med* 15(11):1318–1321.
14. Saffarzadeh M, et al. (2012) Neutrophil extracellular traps directly induce epithelial and endothelial cell death: A predominant role of histones. *PLoS ONE* 7(2):e32366.
15. Semeraro F, et al. (2011) Extracellular histones promote thrombin generation through platelet-dependent mechanisms: Involvement of platelet TLR2 and TLR4. *Blood* 118(7):1952–1961.
16. Wang Y, et al. (2009) Histone hypercitrullination mediates chromatin decondensation and neutrophil extracellular trap formation. *J Cell Biol* 184(2):205–213.
17. Wang Y, et al. (2004) Human PAD4 regulates histone arginine methylation levels via demethylimination. *Science* 306(5694):279–283.
18. Li P, et al. (2010) PAD4 is essential for antibacterial innate immunity mediated by neutrophil extracellular traps. *J Exp Med* 207(9):1853–1862.
19. Leshner M, et al. (2012) PAD4 mediated histone hypercitrullination induces heterochromatin decondensation and chromatin unfolding to form neutrophil extracellular trap-like structures. *Front Immunol* 3:307.
20. Nakashima K, Hagiwara T, Yamada M (2002) Nuclear localization of peptidylarginine deiminase V and histone deimination in granulocytes. *J Biol Chem* 277(51):49562–49568.
21. Darrah E, Rosen A, Giles JT, Andrade F (2012) Peptidylarginine deiminase 2, 3 and 4 have distinct specificities against cellular substrates: Novel insights into autoantigen selection in rheumatoid arthritis. *Ann Rheum Dis* 71(1):92–98.
22. Parker H, Dragunow M, Hampton MB, Kettle AJ, Winterbourn CC (2012) Requirements for NADPH oxidase and myeloperoxidase in neutrophil extracellular trap formation differ depending on the stimulus. *J Leukoc Biol* 92(4):841–849.
23. Li P, et al. (2008) Regulation of p53 target gene expression by peptidylarginine deiminase 4. *Mol Cell Biol* 28(15):4745–4758.
24. Dole VS, Bergmeier W, Mitchell HA, Eichenberger SC, Wagner DD (2005) Activated platelets induce Weibel-Palade-body secretion and leukocyte rolling in vivo: Role of P-selectin. *Blood* 106(7):2334–2339.
25. Pinsky DJ, et al. (1996) Hypoxia-induced exocytosis of endothelial cell Weibel-Palade bodies. A mechanism for rapid neutrophil recruitment after cardiac preservation. *J Clin Invest* 97(2):493–500.
26. Ni H, et al. (2000) Persistence of platelet thrombus formation in arterioles of mice lacking both von Willebrand factor and fibrinogen. *J Clin Invest* 106(3):385–392.
27. Denis CV, Wagner DD (2007) Platelet adhesion receptors and their ligands in mouse models of thrombosis. *Arterioscler Thromb Vasc Biol* 27(4):728–739.
28. Asaga H, Nakashima K, Senshu T, Ishigami A, Yamada M (2001) Immunocytochemical localization of peptidylarginine deiminase in human eosinophils and neutrophils. *J Leukoc Biol* 70(1):46–51.
29. Vossenaar ER, et al. (2004) Expression and activity of citrullinating peptidylarginine deiminase enzymes in monocytes and macrophages. *Ann Rheum Dis* 63(4):373–381.
30. Virchow R (1998) *Thrombosis and Emboli (1846–1856)* (Science History Publications, Canton, MA) p vi, 234 pp.
31. Wakefield TW, Henke PK (2005) The role of inflammation in early and late venous thrombosis: Are there clinical implications? *Semin Vasc Surg* 18(3):118–129.
32. Brighton TA, et al.; ASPIRE Investigators (2012) Low-dose aspirin for preventing recurrent venous thromboembolism. *N Engl J Med* 367(21):1979–1987.
33. Becattini C, et al.; WARFASA Investigators (2012) Aspirin for preventing the recurrence of venous thromboembolism. *N Engl J Med* 366(21):1959–1967.
34. Rohrbach AS, Hemmers S, Arandjelovic S, Corr M, Mowen KA (2012) PAD4 is not essential for disease in the K/BxN murine autoantibody-mediated model of arthritis. *Arthritis Res Ther* 14(3):R104.
35. Hemmers S, Teijaro JR, Arandjelovic S, Mowen KA (2011) PAD4-mediated neutrophil extracellular trap formation is not required for immunity against influenza infection. *PLoS ONE* 6(7):e22043.
36. Thévenaz P, Unser M (2007) User-friendly semiautomated assembly of accurate image mosaics in microscopy. *Microsc Res Tech* 70(2):135–146.
37. Hirahashi J, et al. (2006) Mac-1 signaling via Src-family and Syk kinases results in elastase-dependent thrombohemorrhagic vasculopathy. *Immunity* 25(2):271–283.